

Device Optimization for Organic Photovoltaics With CNT Networks as Transparent Electrode

N. Pimparkar^{1*}, M. Chowalla², M. A. Alam¹

¹School of Electrical and Computer Engineering, Purdue University, West Lafayette, IN 47907-1285, USA.

*Phone: (765) 494 9034 Fax: (765) 494 6441 Email: ninad@purdue.edu

²Materials Science and Engineering, Rutgers University, Piscataway, New Jersey 08854

Abstract — Recently, there has been a lot of interest in flexible and high efficiency solar cells due to cost advantages of roll to roll printing. Traditionally, ITO (Indium Tin Oxide) or ZnO (Zinc Oxide) electrodes have been used as top contacts for solar cells because of their reasonable transparency and moderately low sheet resistance. However, these electrodes are not flexible and would undergo breakdown on bending of flexible substrates. Hence, several groups are working on various types of flexible electrodes which have better optical transparency as well as have high electrical conductivity. Among the various options, CNT (Carbon Nanotube) random networks have emerged as a viable alternative to ITO and ZnO, satisfying these constraints and indeed, several types of solar cells⁽¹⁻⁵⁾ have been reported with CNT random networks as back contact. These experimental reports have so far not been complemented by meaningful modeling of CNT networks in solar cells for performance optimization of the solar cell device design. Here, *for the first time* we present comprehensive simulation results for organic excitonic solar cells with CNT networks as back contact that analyzes all elements of the solar-cell within an end-to-end theoretical framework. In our previous work, we have done extensive modeling of the CNT networks for usage as transistor channel material^(6, 7) and here we use the previously established techniques to model CNT networks as

electrodes. Our analysis shows that optimizing the CNT density is critical to achieve the best tradeoff of transparency vs. over all efficiency of the solar cell.

Fig. 1 shows the simplified schematic of an organic excitonic solar cell and various aspects involved in the modeling and the different pieces of the puzzle are: (a) Exciton generation, (b) Exciton diffusion and dissociation, (c) Charge transport, collection and charge transport through the random CNT network. Below we describe step by step modeling of all these parts and the relevant efficiencies involved.

(a) Exciton generation: Some of the incident light is absorbed by the CNT electrode depending on the electrode transmission which can be modeled by a simple empirical formula as shown in Fig. 2⁸

$$T = T_0 - kD \quad (1)$$

Here the tube density (D) is the number of tubes $/\mu\text{m}^2$, the transmission of substrate is $T_0 = 94\%$ and the constant $k = 0.8\%$. Due to low dielectric constant, an incident photon generates an exciton (or bounded electron hole pair) in an organic material instead of free electron hole pair. An exciton is a charge less particle and diffuses through the organic material. The unstable excitons recombine quickly and hence typically have low exciton diffusion lengths of $L_e \sim 20\text{-}30\text{ nm}$.

(b) Exciton diffusion and dissociation: To separate or dissociate an exciton into an electron-hole pair, a very high electric field is usually necessary. This high electric field is typically present at the interface of two heterostructure materials (e.g. P3HT : PCBM,^{9, 10}) and the exciton must diffuse to such an interface before recombining. Since the exciton diffusion length is typically small, only excitons

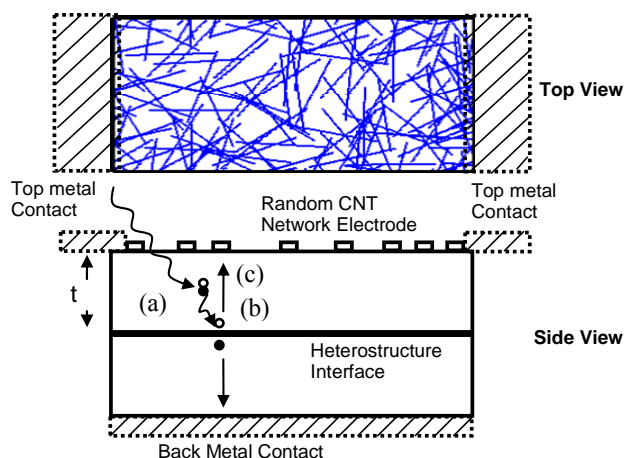


Fig. 1: Geometry organic solar cell with random network of CNT as back contact. The process of solar cell action can be divided as following: (a) Exciton generation, (b) Exciton diffusion and dissociation, (c) charge transport, collection and transport through the random CNT network.

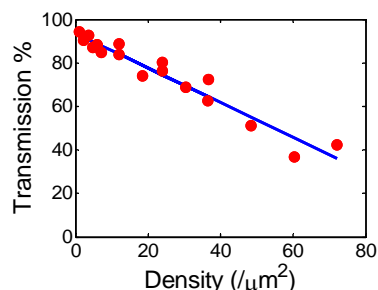


Fig. 2: Transparency vs. Tube density (D) for CNT network electrode. The symbols show experimental data from⁸ and the line shows empirical relation described by Eq. (1)

generated in the active region (region of width $\sim L_e$ near to the interface) get dissociated into an electron-hole pair. Here, we model the exciton diffusion with a simple 1D diffusion equation as excitons are charge less particles and we also include the effect of light absorption length ($L_a \sim 80\text{-}100$ nm) in the model as below,

$$D_e \frac{d^2 e_x}{dx^2} = \frac{1}{\tau_e} (e_x - e_{x0}) - G \quad (2)$$

where, D_e is exciton diffusion coefficient, e_x is exciton concentration, τ_e is exciton recombination lifetime and G is light generation term. The excitons recombination length is given by $L_c = \sqrt{D_e \tau_e}$. Fig. 3 shows the normalized electron-hole pair generation rate as a function of organic layer thickness (t) for various values of L_c and L_a . The results show that the optimal device thickness or the width of the active region is $L_{\max} \sim L_c$. If $t < L_{\max}$, the organic layer is too thin and enough excitons are not generated while for $t > L_{\max}$, the light intensity in the active region drops exponentially while the width of active region remains constant.

(c) Charge transport and collection: After dissociation into free carriers, the charges have to be collected by the electrodes and flown to the outside world. Here, we model the charge transport and charge collection self consistently using the device simulator¹¹ using the simple device structure shown in Fig. 4. Here we replaced the CNT layer by a semiconductor with equivalent sheet resistance. Since in this step we essentially want to capture the effects of

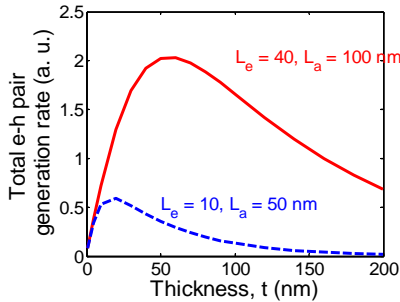


Fig. 3: Normalized electron-hole pair generation rate as a function of organic layer thickness (t) for various values of L_c and L_a (nm). If $t < L_{\max}$, enough excitons are not generated and for $t > L_{\max}$, the light intensity in the active region drops while the width of active region remains constant. The heterostructure interface is at a distance ' t ' from the surface.

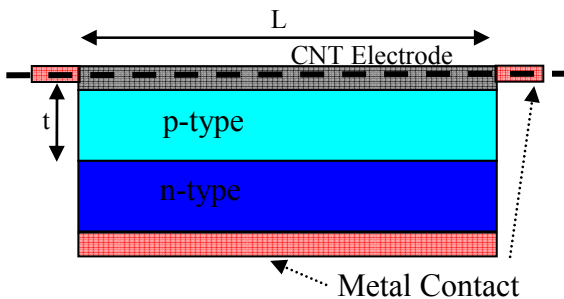


Fig. 4: A simple PN junction solar cell device structure with a thin layer of CNT network with an effective sheet conductance used to simulate the charge transport in device simulator¹¹. Here, t is thickness of active layer and L is length of CNT electrode and the distance between the top metal

charge transport through the semiconductor and the CNT electrode we use a simple PN junction solar cell with a top CNT electrode with contacts on the side as shown in Fig. 4. In this simplified model the effective sheet resistance of the CNT electrode is numerically calculated using the stick percolation model as follows.

Stick Percolation Model:

We constructed a sophisticated first-principle numerical stick-percolation model for the above random CNT network by generalizing the random-network theory. The model¹² randomly populates a 2D grid by sticks of fixed length (L_S) and random orientation (θ) (Fig. 5) and determines I_{ON} through the network by solving the percolating electron transport through individual sticks. In contrast to classical percolation, the CNT network is a heterogeneous network: $1/3^{\text{rd}}$ of the CNTs are metallic and remaining $2/3^{\text{rd}}$ are semiconducting. Since, L_C and L_S are much larger than the phonon mean free path; linear-response transport obviates the need to solve the Poisson equation explicitly. The system is well described by drift-diffusion theory¹² within individual stick segments of this random stick-network. The low bias drift-diffusion equation, $J = qun d\phi/ds$, when combined with current continuity equation, $dJ/ds = 0$, gives the non-dimensional potential ϕ_i along tube i as

$$\frac{d^2 \phi}{ds^2} - C_{ij} (\phi_i - \phi_j) = 0 \quad (3)$$

Here, s is the length along the tube and $C_{ij} = G_0/G_1$ is the

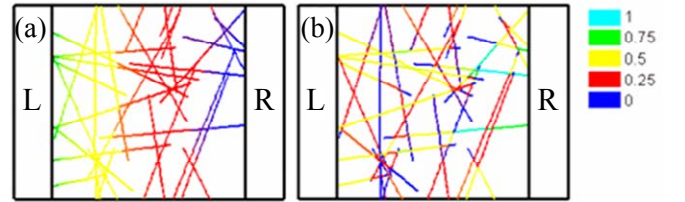


Fig. 5: Normalized potential and current distribution in a random network of CNTs with an applied bias of 1 and 0V on the left and right electrode respectively.

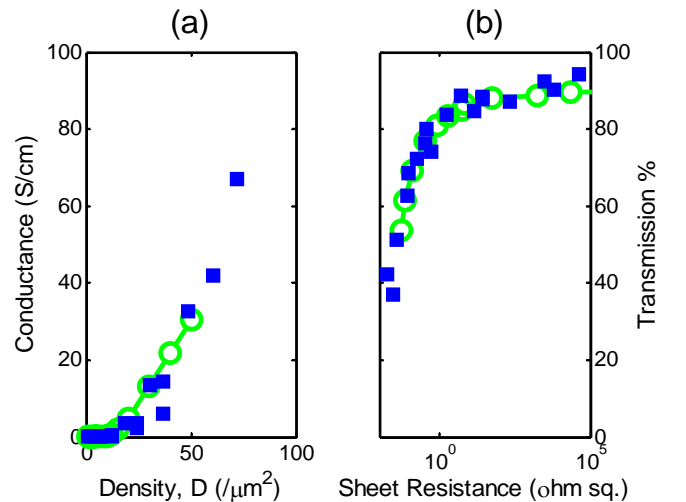


Fig. 6: Experimental⁸ (square blue symbols) and simulated (empty green circles) curves for (a) conductance vs. tube density, and (b) transmission vs. sheet resistance for random CNT networks computed using the stick percolation model. The figure (b) is obtained by combining the results of Fig. (a) and Fig. (2) or the empirical relation in Eq. (1)

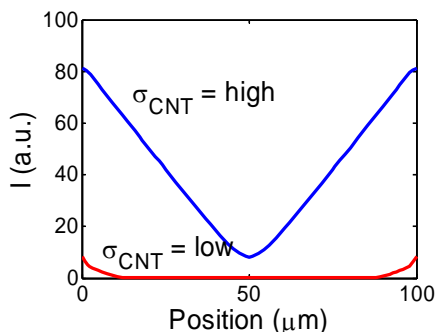


Fig. 7: The current profile along the dotted line in Fig. 4. The blue and red curves show the current profile for high and low density CNT networks. Here, both networks are assumed to have equal transparency.

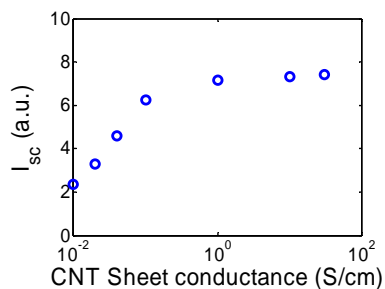


Fig. 8: Normalized short circuit photo current as a function of CNT electrode sheet conductance from device simulator¹¹ results. Comparing with Fig. 6 (a), we see that the photocurrent saturates or maximum current collection is achieved even for moderate values of sheet conductance or tube density.

dimensionless charge-transfer coefficient between tubes i and j at their intersection point, and G_0 ($\sim 0.1 e^2/h$)¹³ and G_1 ($= qn\mu/\Delta x$)¹² are mutual- and self-conductance of the tubes, respectively. Here, n is carrier density, μ is mobility and Δx is grid spacing. The density (D) of the random stick network is measured in $/\mu\text{m}^2$ and the density at which the network starts conducting is defined as percolation threshold (D_{perc}) and is $\sim 5.717 /\mu\text{m}^2$ for random network. The random network was simulated using the above stick percolation model and Fig. 6(a) shows the numerical and experimental⁸ conductance vs. tube density. Combining the results of Fig. 2 (or the empirical relation in Eq. (1)) and Fig. 6(a), we can obtain the transmission vs. sheet resistance.

The final piece of the puzzle is the effects of solar cell dimension. The solar cell length (L) or the distance between the top metal contacts in Fig. 4 can possibly affect the charge collection efficiency as shown in Fig. 7 which is current profile along the dotted line in Fig. 4. When the CNT electrode is highly conductive or has high density, almost all the holes generated at the p-n junction find a path to the metal contacts as shown in Fig. 7, blue curve. The ‘V’ shaped curve suggests that there is little or no current at the midpoint due to symmetry and the total current builds linearly as expected towards the device edge. However, for a less conductive CNT electrode or low density CNT random network, only the holes generated at the edge of the device find a path to top metal contact as suggested by the wide ‘U’ shaped red curve (Fig. 7) reducing the overall current collection efficiency.

Fig. 8 shows the device simulator¹¹ results for different density CNT random network electrodes. Combining these

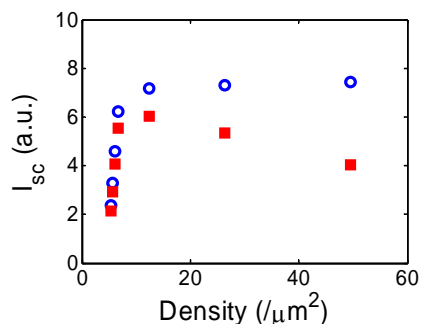


Fig. 9: Normalized short circuit current vs. tube density assuming fully transparent CNT electrode (empty blue circles) and after taking into account the partial opacity of CNT network (filled red squares).

results with Fig. 6 (a), we see that the photocurrent saturates or maximum current collection is achieved even for moderate values of sheet conductance (σ) or tube densities (D). These results suggest that having a very high tube density may not be critical for better charge collection. On the other hand high density CNT network might be counter productive as the transparency of CNT network decreases linearly with the density. Combining all the above pieces (Fig. 2, 6 and 8) in Fig. 9 which shows short circuit current vs. tube density (red filled squares), our simulations show that the optimal density of tubes is about two to three times the percolation threshold (D_{perc}) of the CNT network.

In summary, we for the first time present comprehensive simulation results for organic excitonic solar cells with CNT networks as back contact. We provide an end-to-end theoretical framework that analyzes all elements of the solar-cell. Our simulation results show that a very dense CNT network is not required and in fact degrades the solar cell performance and optimizing the CNT density is critical to achieve the best tradeoff of transparency vs. over all efficiency of the solar cell.

References

- [1] I. Robel, et al., *Advanced Materials* 17, 2458 (2005).
- [2] M. A. Contreras, et al., *Journal of Physical Chemistry C* 111, 14045 (2007).
- [3] T. M. Barnes, et al., *Physical Review B* 75 (2007).
- [4] T. M. Barnes, et al., *Applied Physics Letters* 90 (2007).
- [5] J. van de Lagemaat, et al., *Applied Physics Letters* 88 (2006).
- [6] N. Pimparkar, et al., *Electron Device Letters* 28, 157 (2007).
- [7] N. Pimparkar, et al., *IEEE Transactions of Electron Devices* 54, 637 (2007).
- [8] H. E. Unalan, et al., *Nano Letters* 6, 677 (2006).
- [9] C. Li, et al., *Journal of Materials Chemistry* 17, 2406 (2007).
- [10] A. D. Pasquier, et al., *Applied Physics Letters* 87 (2005).
- [11] Medici, Two Dimensional Device Simulation Program. Synopsis; Version 2003.06 (2003).
- [12] S. Kumar, et al., *Physical Review Letters* 95, 066802 (2005).
- [13] M. S. Fuhrer, et al., *Science* 288, 494 (2000).